Holographic Fabry–Perot spectrometer

Ó. Martínez-Matos,[1,*] José A. Rodrigo,[2] P. Vaveliuk,[1,3] and M. L. Calvo[1]

[1]*Departamento de Óptica, Facultad de Ciencias Físicas, Universidad Complutense de Madrid, Madrid 28040, Spain*

[2]*Instituto de Óptica (CSIC), Serrano 121, Madrid 28006, Spain*

[3]*Facultade de Tecnologia, Servicio Nacional de Aprendizagen Industrial (SENAI)-Cimatec, Avenida Orlando Gomes 1845 41650-010, Salvador, Bahia, Brazil*

**Corresponding author: omartine@fis.ucm.es*

Received October 1, 2010; revised January 18, 2011; accepted January 18, 2011; posted January 21, 2011 (Doc. ID 136030); published February 15, 2011

We propose a spectrum analyzer based on the properties of a hologram recorded with the field transmitted by a Fabry–Perot etalon. The spectral response of this holographic Fabry–Perot spectrometer (HFPS) is analytically investigated in the paraxial approximation and compared with a conventional Fabry–Perot etalon of similar characteristics. We demonstrate that the resolving power is twice increased and the free spectral range (FSR) is reduced to one-half. The proposed spectrometer could improve the operational performance of the etalon because it can exhibit high efficiency and it would be insensible to environmental conditions such as temperature and vibrations. Our analysis also extends to another variant of the HFPS based on holographic multiplexing of the transmitted field of a Fabry–Perot etalon. This device increases the FSR, keeping the same HFPS performance.

OCIS codes: 050.1950, 050.2230, 090.2890, 090.4220, 120.2230, 300.6190.

A Fabry–Perot etalon (FPE) is a well-known device used for very high resolution spectroscopy [1,2]. In spite of its high resolving power, the FPE has some intrinsic disadvantages: (i) the light is mostly reflected when the spectral analysis is performed at one time by means of angular dispersion, avoiding the etalon's tuning; (ii) the free spectral range (FSR) is usually low; and (iii) the response of the etalon is very sensitive to mirrors' misalignment and to environmental conditions such as temperature and vibrations. In this Letter we theoretically compare the features of the FPE with those of the proposed HFPS, which is able to overcome the main disadvantages of the conventional etalon.

Consider an etalon composed of two parallel mirrors with reflectivity coefficients R, separated by an optical spacing, d [3]; see Fig. 1(a). The transmittivity, Γ, of a lossless etalon when it is illuminated by spherical wavefronts arising from an ideal point source, A, is [1]:

$$\Gamma = (1 + F \sin^2 \delta/2)^{-1}, \tag{1}$$

where $F = 4R/(1-R)^2$, $\delta = 4\pi d \cos\theta/\lambda$ is the phase difference between two consecutive reflections, θ is the angle of a ray emanating from A, and λ is the wavelength of the light. Sharp peaks appear at the back focal plane of a convergent lens when $\cos\theta = n\lambda/2d$ (n is an integer). The symmetry of revolution of the system gives rise to a fringe pattern consisting of concentric rings, each one corresponding to a particular value, n. By definition, the resolving power RP, for $\theta \ll 1$, satisfies

$$RP = \lambda/\Delta\lambda = \pi d\sqrt{F}/\lambda, \tag{2}$$

where $\Delta\lambda$ is the incremental wavelength resolved by the etalon. The FSR in which the Fabry–Perot etalon resolves the spectrum without ambiguity, $\Delta\lambda_{\mathrm{FSR}}$, is

$$\Delta\lambda_{\mathrm{FSR}} = \lambda^2/2d, \tag{3}$$

and the number of resolved wavelengths, $\mathcal{F}$, in the interval $\Delta\lambda_{\mathrm{FSR}}$ is called the Finesse:

$$\mathcal{F} = \Delta\lambda_{\mathrm{FSR}}/\Delta\lambda = \pi\sqrt{F}/2. \tag{4}$$

$\mathcal{F}$ is a fixed value (R is fixed) that gives a measure of the spectral sharpness of the etalon. An increase in the resolving power changing d necessarily reduces the FSR. This fact determines the applications of a Fabry–Perot etalon. An alternative analysis of the etalon's spectral response can be done just by considering the interference of the wavefronts emanating from A and the virtual sources A', A''… (separated by a distance, $2d$), as depicted in Fig. 1(a). This approach will be used to characterize the HFPS.

Consider a hologram recorded by the interference of a plane wave (reference beam) with the light transmitted by a Fabry–Perot etalon (object beam). The holographic principle [4] states that the light diffracted by the Fabry–Perot hologram will reconstruct the object beam when it is illuminated by the reference beam. The hologram behaves as a source of a virtual etalon; thus, the diffracted light shows a pattern of concentric rings at the back focal plane of a convergent lens after reconstruction. As the hologram is illuminated with a wavelength, λ, different from the recording one, λ_r, the angular dispersion arising from diffraction also creates a pattern of concentric rings at the back focal plane but shifted accorded to the direction of dispersion. The intensity pattern of a polychromatic light will be smudged, and this setup cannot be used to perform spectral analysis. To bypass this adverse effect, a polychromatic plane wave diffracted by a volume plane grating is used as the input on the Fabry–Perot hologram. If both holograms have the same spatial period and they are set in a parallel arrangement, the Bragg angle on each plate has the opposite sign. Thus the overall device compensates the angular displacement of the rings' centers. In other words, the point sources A, A', A''… associated with each wavelength at reconstruction lie on the same line but in different positions, giving rise to a polychromatic pattern of concentric rings whose radii depend on wavelength. The optical system composed by the two holograms emulates the spectral

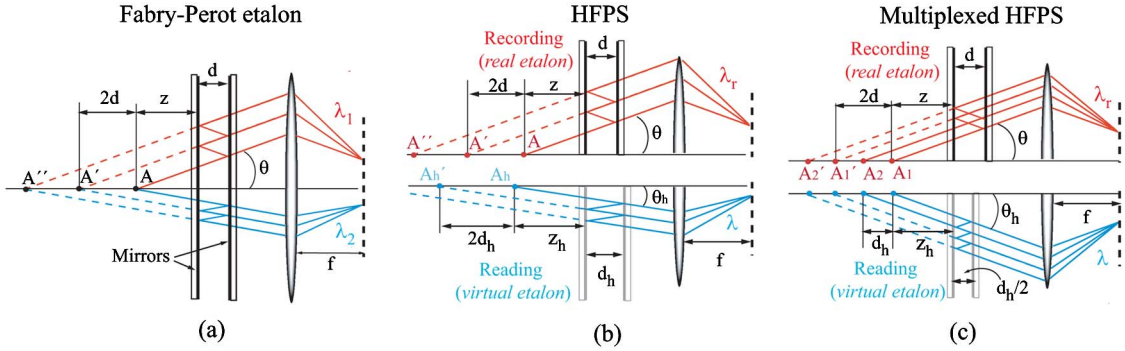

Fig. 1. (Color online) (a) Fabry–Perot etalon illuminated with two spectral components (λ_1 and λ_2) emanating from A. (b) HFPS: top, upper part of the real etalon for holographic recording with λ_r; bottom, down part of the virtual etalon for reconstruction with λ; (c) multiplexing HFPS ($m = 2$): top, upper part of the real etalon for the recording with λ_r; bottom, down part of the effective virtual etalon for reconstruction with λ.

response of the etalon and constitutes the HFPS proposed in this work. Dispersion analysis of parallel gratings can be found in [5].

Ideal point sources A, A', A''… in the recording process, separated a distance, $z + 2jd$, from the left mirror of the etalon, have a different origin, $z_h + 2jd_h = (z + 2jd)\lambda_r/\lambda$, taken from the left mirror of the virtual etalon when the HFPS is illuminated with $\lambda \neq \lambda_r$. The subscript h denotes hologram and j is a positive integer. The ray analysis at the etalon used for hologram recording (top, λ_r) and the ray analysis at the virtual etalon (bottom, λ) at reconstruction of the HFPS are shown in Fig. 1(b). The optical spacing of the virtual etalon, $d_h = d\lambda_r/\lambda$, is wavelength-dependent, and the phase difference between two successive virtual reflections is $\delta_h = 4\pi\lambda_r d\cos\theta_h/\lambda^2$. The expression Eq. (1) still defines the transmittivity of the HFPS, just changing δ by δ_h. The transmittivity peaks occur when incident angles, θ_h, on the virtual etalon [see Fig. 1(b)] satisfy $\cos\theta_h = n\lambda^2/2d\lambda_r$, giving rise to a concentric rings pattern whose radii are wavelength-dependent. This dispersion is the operational principle of the spectrometer proposed. It is straightforward to demonstrate that the dependence of δ_h on λ^{-2} modifies the resolving power, the free spectral range, and the Finesse as follows:

$$\mathrm{RP}_h = \lambda_r/\Delta\lambda_h = 2\pi d\sqrt{F}/\lambda_r, \tag{5}$$

$$\Delta\lambda_{\mathrm{FSR},h} = \lambda^2/4d, \tag{6}$$

$$\Delta\lambda_{\mathrm{FSR},h}/\Delta\lambda_h = \mathcal{F}. \tag{7}$$

Equations (5)–(7) were derived assuming the paraxial approximation $\theta \ll 1$, for which aberrations of the reconstructed wavefronts are negligible. As we can see, the resolving power of the HFPS is increased twice with regard to the etalon, and the free spectral range is reduced to one-half, keeping the Finesse constant. Therefore, a Fabry–Perot etalon with double thickness behaves like the HFPS, except in the throughput of the device. The intensity relation between the input and output light of the HFPS is defined by the product of the holograms' diffraction efficiencies. High performance holographic glass photopolymer [6] could be used to fabricate plane gratings with diffraction efficiencies close to 1. The Fabry–Perot hologram can be recorded using multiple coherent point sources, A, just by illuminating a diffuser located at an anterior position with regard to the etalon. This setup maintains the spectral response of the HFPS with the advantage of a significant increase in the diffraction efficiency. Thus, the HFPS could be fabricated with transmittivity close to 1, being suitable for spectral analysis of weak light sources for chemical, medical, and biological sensing. In contrast, spherical wavefronts impinging on the etalon are mostly reflected when the analysis of the whole spectrum is performed at one time by angular methods. This situation is aggravated for high resolution spectroscopy in which the reflectivity could be $R \sim 0.99$. Besides, the response of the HFPS would be insensitive to a small misalignment between the plane grating and the Fabry–Perot hologram, in comparison with the critical dependence of the alignment between the two mirrors of the etalon. Moreover, temperature variations in the surroundings of the HFPS do not necessarily change the spectral response because the holograms "freeze" in time the optical field at the output of the etalon. These advantages are crucial to practical applications.

We generalize the proposed device to one composed by a volume plane grating and a multiplexed Fabry–Perot hologram. Consider a point, A_1, from which the light is emitted to illuminate the Fabry–Perot etalon. Record m superimposed holograms displacing the source, A_1, distances equal to $2d/m$ and call the new emitting points for each recording A_m. The upper section of Fig. 1(c) shows the ray analysis at the etalon used for hologram recording (top, λ_r) for $m = 2$. If the holograms are recorded under the same experimental conditions, the transmittivity of the multiplexed HFPS would be the coherent addition of the transmitted field by each of the multiplexed virtual etalons. This is a similar condition as for the holographic interferometry procedure. Notice that the multiplexed HFPS's response is different than that of a device composed of two Fabry–Perots working in parallel in which the total transmittivity would be the product of each Fabry–Perot transmittivity. An accurate description of the multiplexed HFPS can be done by considering just one virtual etalon with an effective optical spacing, $d_{\mathrm{ef}} = d\lambda_r/m\lambda$, and an effective reflectivity coefficient, $R_{\mathrm{ef}} = R^{1/m}$. The ray analysis at the effective virtual etalon (bottom, λ) in the reconstruction process is shown in Fig. 1(c). The transmittance of the multiplexed HFPS can be approximated by Eq. (1) replacing δ by

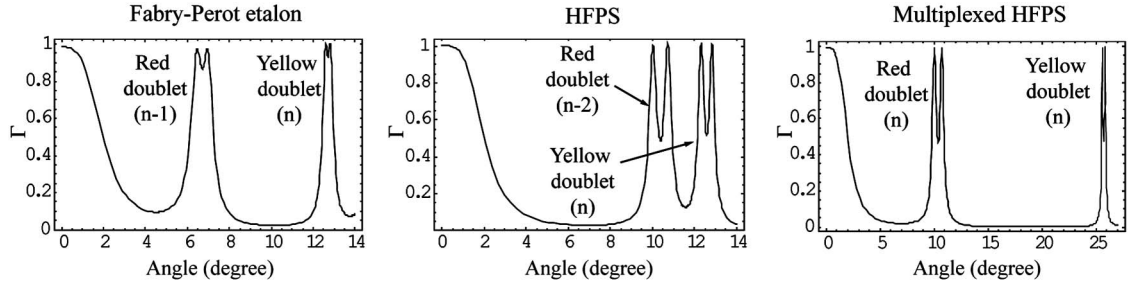

Fig. 2. Simulated transmittivity, Γ, for the yellow and red doublets of a low pressure sodium-vapor lamp analyzed using (a) conventional Fabry–Perot etalon, (b) HFPS, and (c) multiplexed HFPS with $m = 4$. $R = 0.85$, and $d = 12\,\mu$m.

$\delta_{h,m} = 4\pi\lambda_r d\cos\theta_h/m\lambda^2$ and R by R_{ef}. In this case the effective Finesse is $\mathcal{F}_{\mathrm{ef}} = \pi\sqrt{F_{\mathrm{ef}}}/2$, where $F_{\mathrm{ef}} = 4R^{1/m}/(1 - R^{1/m})^2$. $\mathcal{F}_{\mathrm{ef}}$ presents an approximately linear dependence on m, i.e., $\mathcal{F}_{\mathrm{ef}} = \mathcal{F}m$. Moreover, the operational characteristics of the multiplexed HFPS are still described by Eqs. (5)–(7), but now the right hand sides of Eqs. (6) and (7) are given by $m\lambda^2/4d$ and $\mathcal{F}m$, respectively. Hence one may notice that the resolving power is twice the one corresponding to the etalon, and the free spectral range is increased by a factor of $m/2$.

To show an illustrative example, let us analyze theoretically the spectral lines for the yellow-doublet (589.0 nm and 589.6 nm) and the red-doublet (615.4 nm and 616.1 nm) of a low pressure sodium-vapor lamp, considering a conventional etalon with $R = 0.86$ and $d = 12\,\mu$m. This spectrometer cannot resolve the sodium-vapor lamp doublets because the resolution is $\Delta\lambda = 0.7$ nm. The theoretical transmittivity is shown in Fig. 2(a), where the relation between the interferential orders (n and $n - 1$) corresponding to each doublet is explicitly given showing crosstalk, $\Delta\lambda_{\mathrm{FSR}} = 14.7$ nm. The spectral response of the HFPS using the same parameters is shown in Fig. 2(b). One observes that the spectrometer can now resolve each doublet, $\Delta\lambda_h = 0.35$ nm, but there is still crosstalk between the yellow and red emissions, $\Delta\lambda_{\mathrm{FSR},h} = 7.36$ nm. The transmittivity for a multiplexed HFPS with $m = 4$ is shown in Fig. 2(c). This spectrometer resolves the doublets, $\Delta\lambda_h = 0.35$ nm, without ambiguity because $\Delta\lambda_{\mathrm{FSR},h} = 29.45$ nm. This example clearly shows an improvement in the resolving power and free spectral range of a multiplexed HFPS in comparison with the etalon used to record the holograms.

We presented the operational demonstration of two holographic Fabry–Perot spectrometers, a simple hologram HFPS ($m = 1$), and a multiplexed HFPS ($m > 1$). In contrast to the results obtained with the conventional etalon, the HFPS increases both the resolving power, by a factor of two, and the free spectral range, by a factor of $m/2$. Hence, a HFPS with $m > 3$ improves both spectral characteristics. In addition, because the holograms can be recorded into a highly efficient photopolymerizable glass [6], the proposed device could be fabricated to be highly efficient and its spectral response to be less sensitive to small misalignments and to environmental changes.

We thank A. Cámara Iglesias for valuable discussions and advice. Financial support from the Spanish Ministry of Science and Innovation under project TEC 2008-04105 is acknowledged. P.Vaveliuk acknowledges Conselho Nacional de Desenvolvimento Científico e Tecnológico (CNPq), Brazil, for financial support.

References

1. M. Born and E. Wolf, *Principles of Optics* (Cambridge University, 1999).
2. J. M. Vaughan, *The Fabry–Perot Interferometer: History, Theory, Practice and Applications* (Taylor & Francis, 1989).
3. Ch. Fabry and A. Perot, Ann. Chim. Phys. **7**, 459 (1897).
4. L. Solymar and D. J. Cooke, *Volume Holography and Volume Gratings* (Academic, London, 1981).
5. O. Martinez-Matos, J. A. Rodrigo, M. P. Hernández-Garay, J. G. Izquierdo, R. Weigand, M. L. Calvo, P. Cheben, P. Vaveliuk, and L. Bañares, Opt. Lett. **35**, 652 (2010).
6. F. del Monte, O. Martínez-Matos, J. A. Rodrigo, M. L. Calvo, and P. Cheben, Adv. Mater. **18**, 2014 (2006).